

Arteriovenous crossing in retinal vessels of mice, rats, and pigs

Gottfried Martin, Kira L. Wefelmeyer, Felicitas Bucher, Günther Schlunck, Hansjürgen T. Agostini

Eye Center, Medical Center, Medical Faculty, University of Freiburg, Freiburg, Germany

Purpose: Retinal vein occlusions (RVOs) are a common disease, but there are no animal models for spontaneous RVO formation. The critical sites of predilection, especially for branch RVO (BRVO), are the arteriovenous crossing sites in the inner retina. To gain more insight into possible animal models, the anatomic structure of retinal arteriovenous crossings was investigated in mice, rats, and pigs and compared to the human situation.

Methods: Retinal flat mounts and paraffin sections of eyes from mice, rats, pigs, and humans were stained with GS lectin, Masson's trichrome, or immunohistochemistry for ACTA2 and GFAP. Serial sections of arteriovenous crossing sites were investigated.

Results: Mice usually do not show retinal arteriovenous crossings. Rats have a mean of 2.8 ± 1.4 crossings per eye at a mean distance from the optic nerve head of 2.79 ± 0.53 mm, though the diameters of the crossing vessels are small. The situation in pigs is similar to that in humans, with many arteriovenous crossings of vessels and with similar diameters as found in humans. A mean of 28.4 ± 3.5 crossings per retina was found, and 23% of these were arterial overcrossings. Serial paraffin sections showed that the tunica media of the artery touched that of the vein, but they did not fuse.

Conclusions: While the retinal arteriovenous crossings of mice and rats are absent or comprised of rather thin vessels, those in the porcine retina are similar to adult humans. Therefore, the porcine retinal vascular bed may serve as a model to assess early steps in the formation of RVOs.

Retinal vein occlusion (RVO) is a common disease in industrialized countries. Though there are several opinions on how the occlusion develops [1,2], there are only sparse experimental data. As RVO is not usually treated surgically, tissue specimens for laboratory investigations are rare. Therefore, animal models are essential to understand the conditions and the process of RVO formation.

Fundus observations in patients show that branch RVO (BRVO) typically occurs at arteriovenous crossings [3,4], while central RVO (CRVO) occurs within the optical nerve head [5,6]. In human BRVO, the arteriovenous crossing sites were investigated in serial sections showing a close convergence of both vessels with a common adventitia at the crossing site [1,7,8]. In almost all cases of BRVO, the vein resides between the retina and the crossing artery, i.e., the artery is located on top of the vein toward the vitreous. The vein is depressed into the retinal tissue, and its cross section is flattened and broadened to a certain extent. This vascular conformation is a likely cause of turbulent blood flow, which favors thrombus formation. However, surgical separation of the artery and vein after vitrectomy in patients with BRVO did not lead to a significant functional improvement, especially in comparison to intravitreal anti-vascular endothelial

growth factor (VEGF) treatment, and it is not recommended anymore [9].

Current animal models of BRVO depend on experimental occlusion of the vein, either by mechanical means or by robust laser treatment [10,11]. They allow an investigation of the consequences of an RVO, such as hypoxia, microglial activation, and inflammation. They also allow the testing of surgical or therapeutic strategies in porcine models [12-14]. In contrast, they do not allow observation of RVO formation. For this purpose, an animal model is favorable where the occlusion is induced by food, pharmacological treatment, or genetic conditions. To select such an appropriate model organism, it is important to characterize the anatomic and histological structure of the arteriovenous crossing sites in the respective species. Whereas vascular corrosion casts were studied in rats and pigs [15,16], in this study, we investigated the histology of arteriovenous crossings in the retina of rats and pigs by serial paraffin sections and compared to those of a human specimen.

METHODS

Animals and human specimen: Six eight-week-old C57BL/6J mice and Sprague-Dawley rats of the same age were used. They were housed at 24 °C with a 12 h:12 h light-dark rhythm. The eyes were gifts from collaborating groups working with different organs (brain or lung). Eyes from pigs were freshly obtained from a local abattoir. Mice were perfused with PBS (9.1 mM Na_2HPO_4 , 1.7 mM NaH_2PO_4 ,

Correspondence to: Gottfried Martin, Universitätsklinikum Freiburg, Klinik für Augenheilkunde, Killianstr. 5, 79106 Freiburg, Germany; Phone: ++49-76127040010; email: gottfried.martin@uniklinik-freiburg.de

150 mM NaCl, pH 6.8) after death, while rats were not. All animal procedures adhered to the animal care guidelines of the Institute for Laboratory Animal Research (Guide for the Care and Use of Laboratory Animals) in accordance with the ARVO Statement for the Use of Animals in Ophthalmic and Vision Research, and they were approved by the local animal welfare committee (Tierschutzkommission).

A human retinal specimen from an eye that was enucleated due to a uveal carcinoma was used for comparison (female, 72 years). Institutional Review Board (IRB)/Ethics Committee approval had been obtained for specimen acquisition and use and data generation.

Retinal flat mounts: Eyes from mice or rats were fixed in 4% formalin for 1–2 h and then transferred to PBS. After a circumferential cut, the anterior part of the eye was removed and the retina was immersed in PBlec (1 mM CaCl₂, 1 mM MgCl₂, 10 g/l BSA in PBS). GSL1-Lectin labeled with TRITC was added to a final concentration of 5 µg/ml, and the retinas were incubated at 4 °C overnight. After washing, the retinas were mounted on slides.

Paraffin sections: Eyes from rats were fixed in 4% formalin for 1–2 h and then transferred to PBS. After removing the anterior part including the lens, five sclera and retina cups were arranged as a stack in a small reaction tube in 2% agarose in PBS liquefied at 60 °C. First, some agarose was filled into the tube. Then, a cup was put at the top of the agarose and embedded with additional agarose. This procedure was repeated five times. The agarose block was then embedded in paraffin.

Porcine eyes were freed from adherent tissue and opened by a circumferential cut to remove the anterior part of the eye, including the lens and vitreous. The optic nerve head was cut out by a 6 mm punch. The rest of the posterior part of the eye, including the retina and sclera, was cut into three parts for easier handling. The retina was carefully removed and submerged in PBS. Sites of arteriovenous crossings were cut out using a scalpel under a dissecting microscope and fixed in 4% formalin. After transfer to PBS, the crossing sites were arranged in parallel in 2% agarose in PBS liquefied at 60 °C by the following procedure. In a small syringe from which the tip was cut off, some agarose was filled in. Then, a crossing site was arranged at the agarose surface and covered with agarose. This procedure was repeated for nine additional crossing sites. After cooling, the agarose block was embedded in paraffin. Serial paraffin sections were stained with Masson's trichrome. The human specimen was treated similarly.

Immunohistochemistry: Paraffin sections from pieces of porcine or human retina were pre-selected for the presence of arteriovenous crossings. Staining was performed by standard procedures. After demasking the sections in boiling Tris-EDTA buffer, primary antibodies (monoclonal mouse anti-vascular smooth muscle actin [ACTA2], clone 1A4, A2547, Sigma, Taufkirchen, Germany, 1:2,000; or polyclonal rabbit anti-glial fibrillary acidic protein [GFAP], RB-087-A0, Thermo Fisher Scientific, Germany, 1:2,000) were followed by biotinylated secondary antibodies, avidin coupled with alkaline phosphatase, and Vector Red AP Substrate Kit I, (Vector Labs, Burlingame, CA). Sections were counterstained with hematoxylin.

RESULTS

Arteriovenous crossings in murine retinas are highly rare: The inner retinal vasculature in mice typically consists of four to six main arteries and four to six main veins (Figure 1A and Appendix 1). Arteries and veins originate from the optic nerve head and extend radially in an almost equiangular alternating fashion. The corresponding areas of arterial and venous capillaries typically do not overlap but are arranged side by side. Sometimes, a small vein has a small area of venous capillaries that does not reach the periphery. In this case, the remaining venous area is drained by a peripheral arc of a neighboring large vein (Figure 1A). The same is true when a larger artery branches so that the venous area between the two branches is drained from a peripheral vein. In this way, the typical murine retina does not show arteriovenous crossings.

Location of retinal arteriovenous crossings in rats and pigs: Although the arrangement of retinal arteries and veins in rats is similar to that in mice, some arteriovenous crossings are present. The distribution of arteriovenous crossings was determined in 29 flat mounted retinas of rats. The mean number of crossings per retina was 2.8±1.4 with a range of 1–5. The mean distance from the optic nerve head was 2.79±0.53 mm with a range of 1.3–3.7 mm, while the distance from the optic nerve head to the border of the retina was around 4.5 mm. This means that most crossings are at a distance of two-thirds of the retinal width from the optic nerve head (Figure 1). Most arteries and veins run radially, alternating in a spoke wheel-like arrangement equivalent to the situation in mice. Therefore, the central part of the retina is sufficiently supplied with blood. However, as the retina of rats is larger than that of mice, not all peripheral venous areas that are located between two arterial branches or between two arteries separated by a short vein are drained by a peripheral arc of a large neighboring vein. Instead, veins are crossing

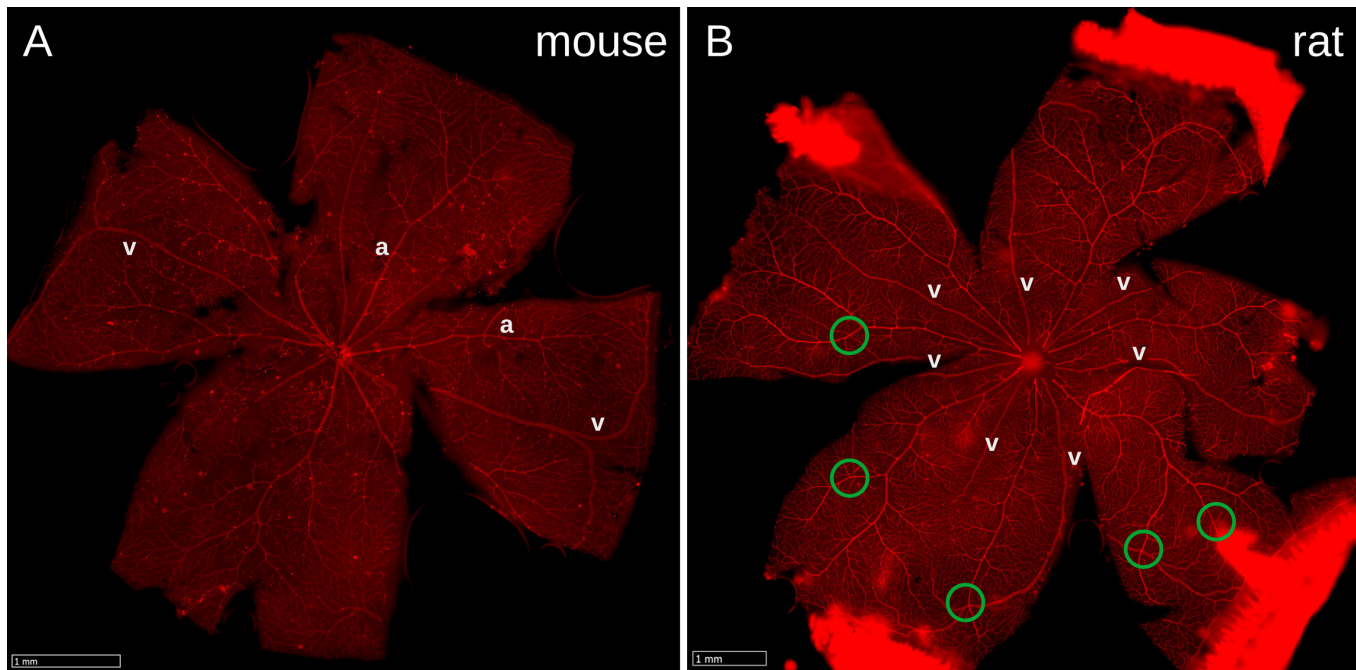


Figure 1. Murine and rat retinal flat mounts. Flat mounted retinas from mice or rats stained with lectin. The main vessels are arranged radially with alternating arteries and veins. **A:** Six arteries (a) are separated by three large and three smaller veins (v) in mice. The two largest veins form three peripheral arcs draining additionally the peripheral areas of the smaller veins without crossing an artery. Arteriovenous crossings are highly rare and are not found in most retinas. **B:** There are some arteriovenous crossings (indicated by green circles) in rats. Most crossings are found at two-thirds the distance between the optic nerve head and the periphery. Usually, the vein is crossing an artery to reach an area between two arterial branches or an area between two arteries with a small and short vein in between.

arteries. Accordingly, more crossings were found in retinas with a small number of veins. The rather large distance of the crossings from the optic nerve head implies that the crossing vessels are rather small in diameter with a thin wall and thus unlikely to form a compressive RVO.

The spatial position of the artery in relation to the vein was determined by carefully focusing the microscope. The artery was above the vein (toward the vitreous) in 44% of the crossings in rats.

In porcine retinas, many arteriovenous crossings were found in a large variety of distances from the optic nerve head (Figure 2). Accordingly, the diameter of the vessels at the crossing sites varied widely. This is similar to the situation in humans. In total, 28.4 ± 3.5 crossings per retina (mean \pm standard deviation) were found in five pig eyes, and $23 \pm 11\%$ of these were arterial overcrossings. Veins dive into the inner layers of the retina at small ramifications, mainly in the periphery. In these cases, it is sometimes difficult to see whether there is a crossing with the artery touching the vein or if it is simply an underpinning with a greater distance of both vessels. As a consequence, the percentage of true arterial overcrossings may be even smaller.

Sections of retinal arteriovenous crossings: Serial paraffin sections were prepared to enable a closer look at the retinal arteriovenous crossing sites. Examples from the rat retina are shown in Figure 3 and Appendix 2 and Appendix 3. At the contact site, the artery and the vein seem to share a common vessel wall. No neuronal tissue was found between both vessels. Arterial overcrossings were observed in three out of nine crossing sites investigated in serial sections. The crossing vessels are rather small in diameter so that the crossings locate to the nerve fiber layer or ganglion cell layer and do not extend to deeper retinal layers, as is the case in larger animals, such as pigs or humans.

The arteriovenous crossing sites of larger vessels in the porcine retina show a typical composition known from human crossing sites. The tunica media layers of the artery and vein are intensely stained blue by trichrome staining (Figure 4, Appendix 4, Appendix 5, Appendix 6 and Appendix 7), or red by immunostaining for ACTA2 (Figure 5 and Appendix 8), and they are in close contact with no neuronal tissue in between, as shown by immunostaining for GFAP, an intermediate filament mainly expressed in astrocytes and also in Müller cells. GFAP staining was outside of this wall, and both formed a sharp border with no intermediate tissue

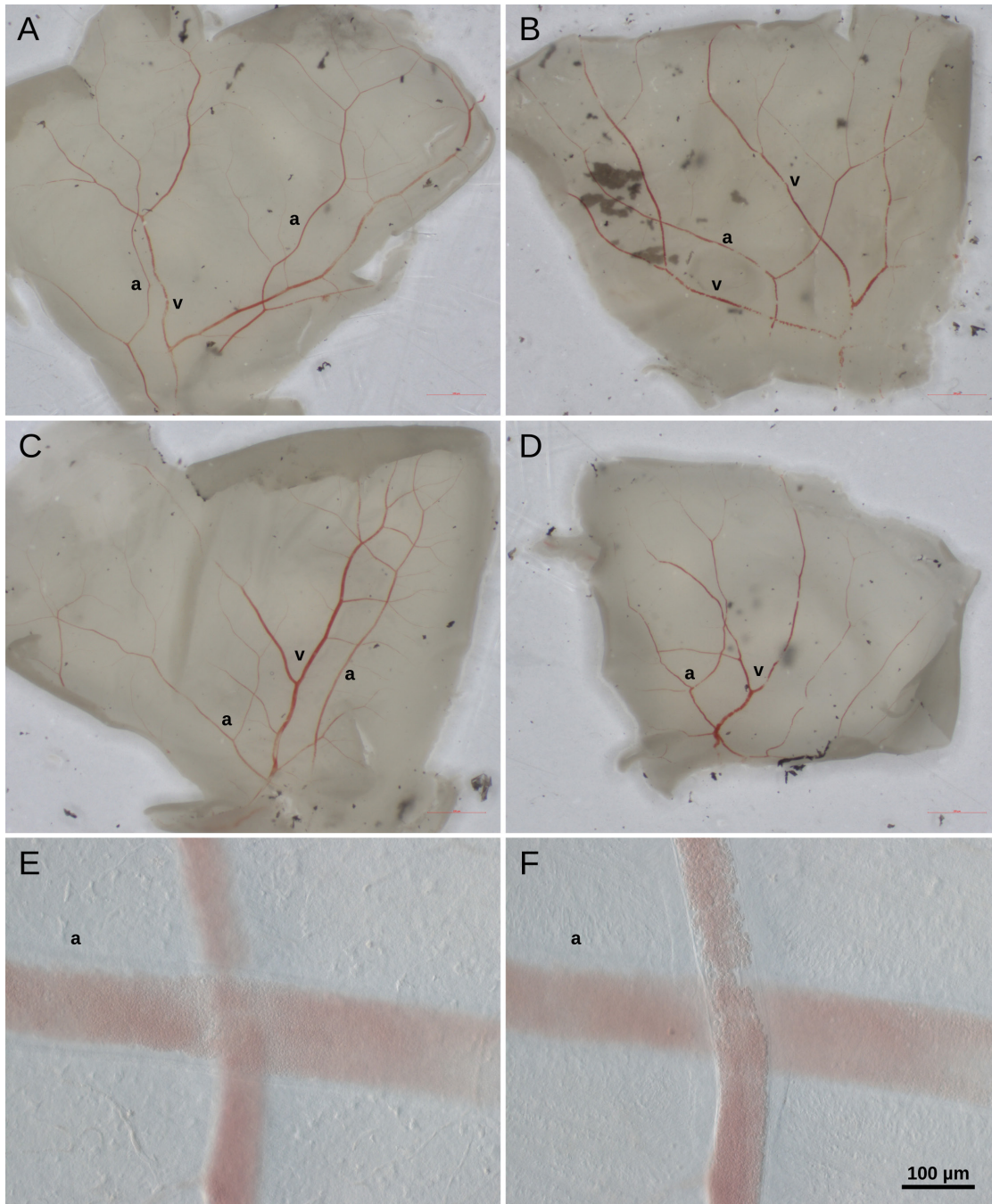


Figure 2. Porcine retinal flat mounts. Pieces of fresh, unfixed, porcine retina in PBS, as seen in a dissecting microscope. Vessels are filled with red blood cells. **A–D**: Many arteriovenous crossings at different distances from the optic nerve head (located at the bottom of each image) are visible. The veins are somewhat thicker than the arteries. **E–F**: Arteriovenous crossing in a flat mounted porcine retina imaged with differential interference contrasts (DICs). **E**: Focus on the thick-walled artery. **F**: Focus on the vein that is crossing above the artery.

(Figure 5). At the center of the arteriovenous crossing site, the media of the artery touched the media of the vein without fusion of both. In some cases, the neuronal tissue around the vessels appears loose so that the vessels may be surrounded by a common tunica adventitia. This is in accordance with a

higher density of astrocytes immunostained by GFAP around the vessels (Figure 5). These features are similar to the human situation (Figure 6, Appendix 9 and Appendix 10).

Some differences between pigs and humans are as follows. While the ACTA2 staining covers the whole

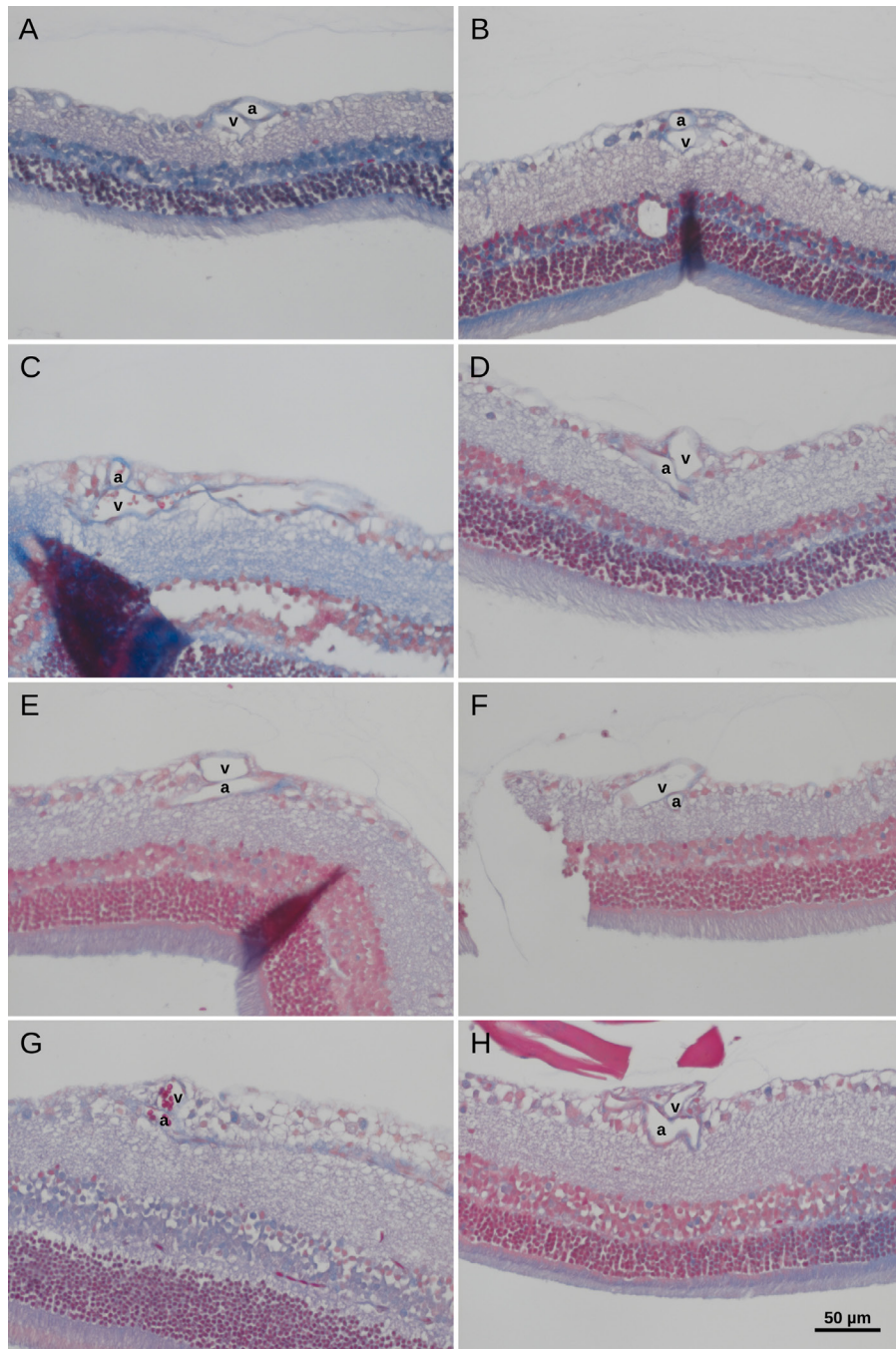


Figure 3. Rat retinal arteriovenous crossings. Paraffin sections of retinal arteriovenous crossings in rats stained with trichrome. Arteries are characterized by a slightly thicker wall and a rounded oval cross-section area. These features are prominent in only some of the serial sections. **A–C**: The artery (a) is above (toward the vitreous) the vein (v); the vein is cut longitudinally in **C**. **D–H**: The vein is crossing over the artery (toward the vitreous). The artery is cut perpendicularly in **F**, while it is cut obliquely in **D**, **E**, **G**, and **H**. At all crossing sites, only a small tissue layer separates artery and vein. No obvious compression of the veins was observed.

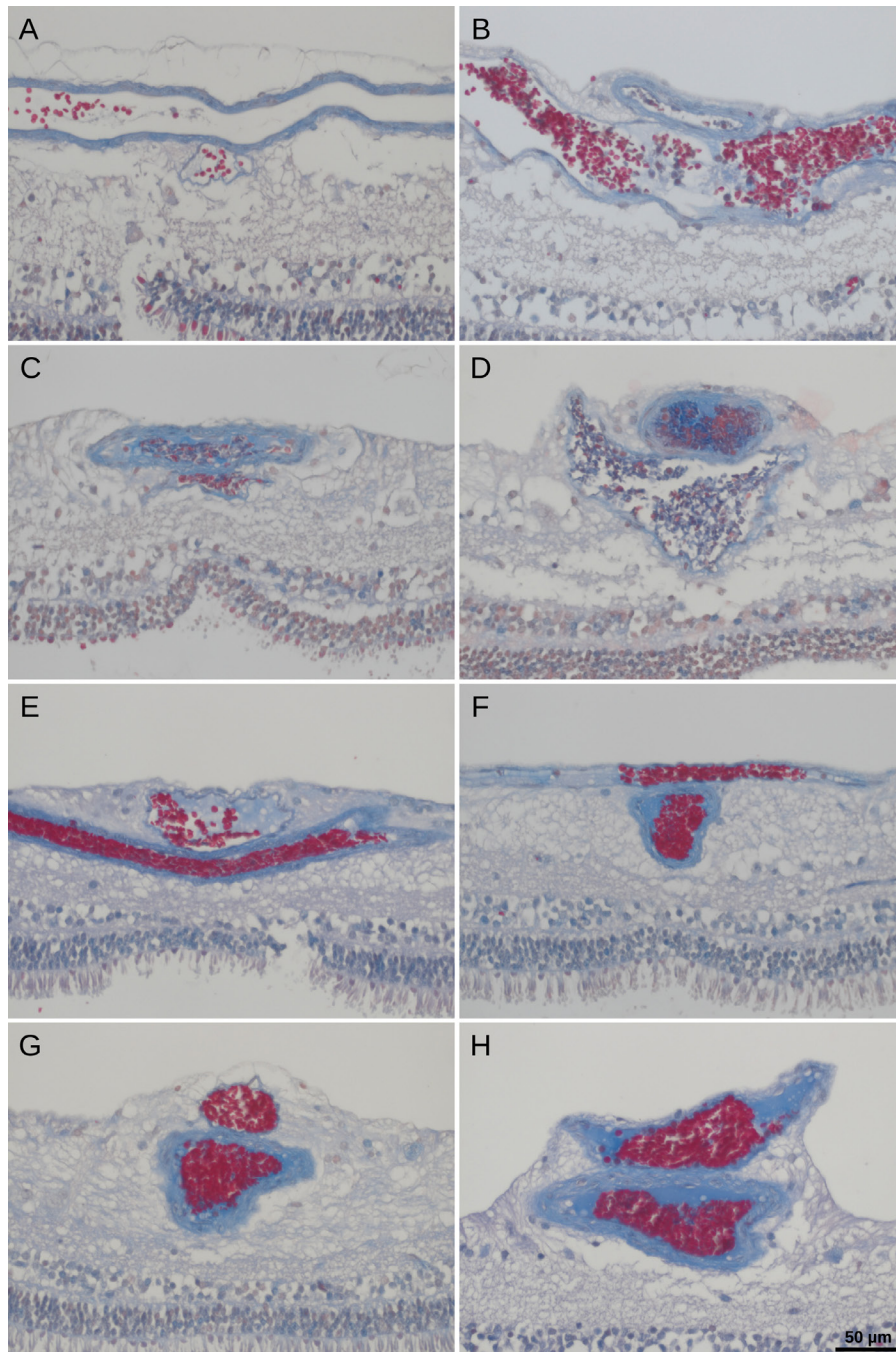


Figure 4. Porcine retinal arteriovenous crossings. Images from serial paraffin sections of porcine retinal arteriovenous crossing sites stained with trichrome. The artery has a much thicker wall (stained blue) and a rounded shape in cross sections as compared to the vein. **A–D**: The artery is crossing above the vein. **E–H**: The vein is crossing above the artery. Large vessels are clearly above the inner retinal level in **B**, **D**, and **H**.

thickness of the porcine media, the staining is restricted to one or (in larger vessels) two rings in the human specimen. The cross-sectional areas and shapes usually did not change at porcine crossing sites. Only in cases where vessel diameters were highly different was some flattening or compression

of the small vessel observed within the crossing area. This flattening was only visible in perpendicular cross sections of the small vessel. In human arterial overcrossings, the artery usually slightly impinges on the vein, resulting in a heart-shaped venous cross section (Figure 6). In addition, porcine

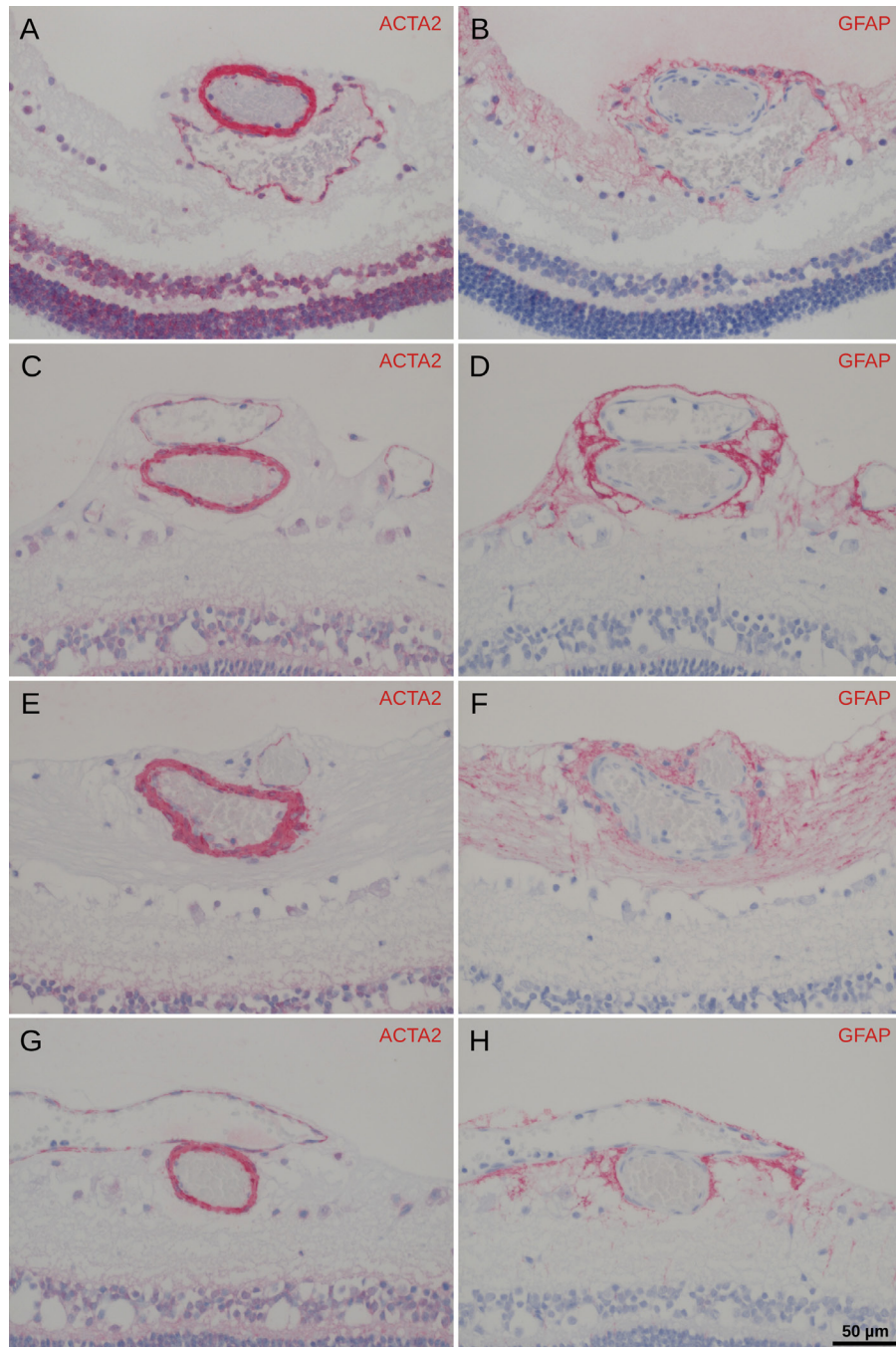


Figure 5. Immunohistochemistry of porcine arteriovenous crossings. Immunohistochemical staining of serial paraffin sections of porcine retinal arteriovenous crossing sites using antibodies raised against ACTA2 (A, C, E, and G) and GFAP (B, D, F, and H). Vicinal sections are compared. While the antibody raised against GFAP stains astrocytes (and some Müller cells) in the nervous tissue surrounding the vessel, the antibody raised against vascular smooth muscle ACTA2 stains the compact layer of the vessel wall that is intensely stained by aniline blue in the trichrome staining. The layers of the vascular wall that are stained by the antibody raised against ACTA2 are touching but not fusing. There is no space left for cells expressing GFAP between the two vessels at the center of the crossing. Note that the astrocytes show a much higher density around the vessels. A and B show the same arterial overcrossing as in Figure 4D.

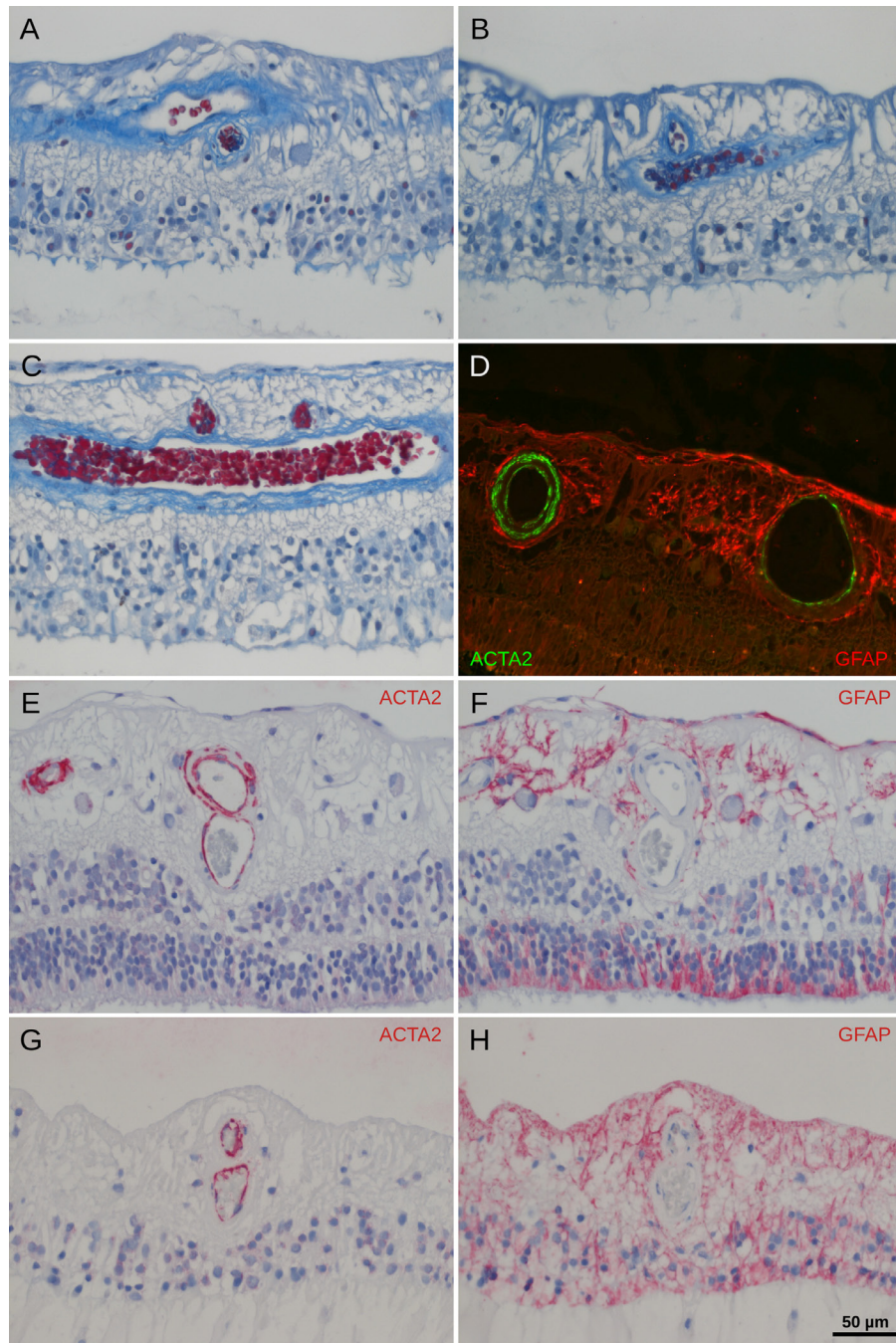


Figure 6. Human arteriovenous crossings. **A–C**: Images from serial paraffin sections of human retinal arteriovenous crossing sites stained with trichrome. The eye was enucleated because of a tumor and shows some alteration from the normal retinal aspect. The vessels are within the inner retinal layers and the vessel wall shows a low density in contrast to pigs. The artery has a slightly thicker wall (stained blue) and a rounded shape in cross sections as compared to the vein. **A–B**: The artery is crossing above the vein. **C**: Two veins that split just before passing the artery are crossing above the latter. **D**: Immunohistochemical staining of a paraffin section of human retina using antibodies raised against ACTA2 and GFAP. In the artery (left) and the vein (right), the GFAP staining is surrounding the tunica media (stained by ACTA2), resulting in a complementary staining pattern that does not overlap. **E–H**: Immunohistochemical staining of serial paraffin sections of human retinal arteriovenous crossing sites using antibodies raised against ACTA2 (**E** and **G**) and GFAP (**F** and **H**). Adjacent sections are compared. The staining is similar to that of porcine crossings. The outer border of the tunica media is more clearly visible than the trichrome staining. Usually, the undercrossing vein shows a depression at the site where it is touching the artery. The layers of the vascular wall that are stained by the antibody raised against ACTA2 are touching but not fusing. **E** and **F**: A large vein is undercrossing a large artery in the central retina. **G** and **H**: A large vein is undercrossing a small vein in a peripheral part of the retina (compare the thickness of the retina).

vessels are positioned more superficially, within the nerve fiber layer and often extending into the vitreal space, whereas the human vessels are running within the ganglion cell layer. At the crossing site, the overlaying porcine vessel, usually the vein, deviates into the vitreal space, whereas the underlying human vessel, usually the vein, deviates toward the outer layers of the retina. Arterial overcrossing was observed in five of 27 (19%) porcine crossing sites investigated by serial sections. In the human specimen, six of seven (86%) crossing sites investigated by serial sections were arterial overcrossings. These differences should be considered when choosing an animal model.

DISCUSSION

RVO is a common disease in industrialized countries, and BRVO is more common than CRVO [17]. BRVO was found to occur at arteriovenous crossing sites and is restricted almost exclusively to arterial overcrossings [4,18].

Arterial overcrossings are more common in humans (67% to 71% of crossings) and are almost exclusive at BRVO sites (97.6%) [4]. In human eyes with BRVO, the arteries at the occlusion site are overlaying the vein toward the vitreous at 99% of arteriovenous crossings, whereas at other crossing sites, the artery is anterior to the vein in around 60% of the crossings [19]. In another study, arteries were anterior to the vein, toward the vitreous cavity, at all BRVO sites in 26 eyes examined, while in a control group, the artery was anterior to the vein 65% of the time [20]. The values of 44% of arterial overcrossings in flat mounts and 33% in retinal sections of rats, as well as 23% of arterial overcrossings in flat mounts and 19% in retinal sections of pigs were somewhat smaller. Similar ratios were reported earlier in studies of retinal vascular corrosion casts for rats [15] and for pigs [16]. The small value for pigs is a feature of the porcine species and must be considered when selecting a model species.

RVOs were reported to occur most commonly in the superotemporal quadrant and second-most commonly in the inferotemporal quadrant of the human retina within a distance of three disc diameters (6 mm) from the optic disc [18,21-23]. In the superotemporal quadrant, a greater proportion of crossings were vein-posterior than in the inferotemporal quadrant [24], which may explain the distribution of RVOs. In pigs, no RVOs were reported, so there is no distribution of occlusion sites. In our study, the distribution of arteriovenous crossings was investigated in retinal flat mounts of rats but not pigs because of high distortions from flattening spherical tissues, and it is unknown if this is relevant to BRVO.

An arteriovenous crossing implicates that both vessels converge. In pigs, the tunica media of the vein and that of the artery touch at the center of the crossing site but do not fuse. There is no space left for neuronal tissue, as indicated by GFAP immunostaining. This fits the situation in humans and is in agreement with earlier histological reports [1,8]. Some of these reports also describe that arteries and veins have a common adventitial sheath at the crossing site. A slightly denser mesh of GFAP-positive filaments was observed in our study in pigs and humans that may be interpreted as a tunica adventitia. Thickening of the tunica media or other layers of the vessel wall at the crossing site, as described in earlier reports [8], was not observed in our study.

At arterial overcrossing sites in humans, the artery is straight while the vein is dipping into the retina to pass under the artery [1,25]. Other studies did not report such retinal vein dipping [3], so it is unclear whether this feature is important to RVO formation. In this study, we observed this feature at arteriovenous crossing sites in humans but not in pigs. In the latter, the artery rather deviates into the vitreous. This is related to the finding that the large vessels near the optic nerve head are on top of rather than within the retina [16]. This porcine feature must be considered when selecting a model species.

A good model species for the study of human RVOs should represent as many of the typical histological features at the arteriovenous crossing site as possible. Important features are the thickness and structure of the vessel walls, as well as the position and course of the vessels within the retina. In addition, it might be worth studying arteriovenous crossings in a primate species that has a macula. The streak-shaped macular area of pigs contains no major vessels, but unlike the central fovea in the human eye, it is not completely avascular [16].

The histological aspect of the arteriovenous crossings in pigs is quite similar to that reported in humans. In contrast, arteriovenous crossings in rats are rare and located more peripherally, resulting in crossings of only small vessels. This is not typical in the human situation. Arteriovenous crossings in mice are usually missing. In conclusion, though a primate model might be an even better choice, the retinal arteriovenous crossings in pigs seem to be attractive sites to observe spontaneously occurring early stages of RVO.

APPENDIX 1. MURINE AND RAT RETINAL FLAT MOUNTS.

To access the data, click or select the words “[Appendix 1.](#)” High resolution images of Figure 1.

APPENDIX 2. RAT RETINAL ARTERIOVENOUS CROSSINGS.

To access the data, click or select the words “[Appendix 2.](#)” Image stack of the serial paraffin sections from fig. 3E. Please, scroll through the series e.g. by using the mouse wheel.

APPENDIX 3. RAT RETINAL ARTERIOVENOUS CROSSINGS.

To access the data, click or select the words “[Appendix 3.](#)” Image stack of the serial paraffin sections from fig. 3F. Please, scroll through the series.

APPENDIX 4. PORCINE RETINAL ARTERIOVENOUS CROSSINGS.

To access the data, click or select the words “[Appendix 4.](#)” Image stack of the serial paraffin sections from fig. 4A. Please, scroll through the series e.g. by using the mouse wheel.

APPENDIX 5. PORCINE RETINAL ARTERIOVENOUS CROSSINGS.

To access the data, click or select the words “[Appendix 5.](#)” Image stack of the serial paraffin sections from fig. 4B. Please, scroll through the series.

APPENDIX 6. PORCINE RETINAL ARTERIOVENOUS CROSSINGS.

To access the data, click or select the words “[Appendix 6.](#)” Image stack of the serial paraffin sections from fig. 4E. Please, scroll through the series.

APPENDIX 7. PORCINE RETINAL ARTERIOVENOUS CROSSINGS.

To access the data, click or select the words “[Appendix 7.](#)” Image stack of the serial paraffin sections from fig. 4F. Please, scroll through the series.

APPENDIX 8. PORCINE RETINAL ARTERIOVENOUS CROSSINGS.

To access the data, click or select the words “[Appendix 8.](#)” Image stack of the serial paraffin sections from fig. 5C. Please, scroll through the series e.g. by using the mouse wheel.

APPENDIX 9. HUMAN RETINAL ARTERIOVENOUS CROSSINGS.

To access the data, click or select the words “[Appendix 9.](#)” Image stack of the serial paraffin sections from fig. 6B stained by trichrome. Please, scroll through the series.

APPENDIX 10. HUMAN RETINAL ARTERIOVENOUS CROSSINGS.

To access the data, click or select the words “[Appendix 10.](#)” Image stack of the serial paraffin sections from fig. 6E stained by immunohistochemistry. Please, scroll through the series.

ACKNOWLEDGMENTS

We thank Prof. Dr. K. Kierdorf for providing mouse eyes and Prof. Dr. S. Schumann and Dr. S. Spassov for providing rat eyes after killing the animals at the end of their respective animal procedures. We thank Marc Guder for excellent technical assistance.

REFERENCES

- Seitz R. Die NetzhautgefäÙe: vergleichende ophthalmoskopische und histologische Studien an gesunden und kranken Augen. Stuttgart: Enke; 1962.
- Tourville E, Schachat AP, Hansen LL, Hoerauf H, Burton M, Gregor Z. u. a. Vascular Occlusive Disease [Internet]. In: Jousseaume AM, Gardner TW, Kirchhof B, Ryan SJ, herausgeber. Retinal Vascular Disease. Berlin, Heidelberg: Springer Berlin Heidelberg; 2007. Seite 424–527.
- Frangieh GT, Green WR, Barraquer-Somers E, Finkelstein D. Histopathologic study of nine branch retinal vein occlusions. Arch. Ophthalmol. Chic. 1982; 100:1132-40. [PMID: 6178389].
- Weinberg D, Dodwell DG, Fern SA. Anatomy of arteriovenous crossings in branch retinal vein occlusion. Am J Ophthalmol 1990; 109:298-302. [PMID: 2309862].
- Green WR, Chan CC, Hutchins GM, Terry JM. Central retinal vein occlusion: a prospective histopathologic study of 29 eyes in 28 cases. Trans Am Ophthalmol Soc 1981; 79:371-422. [PMID: 7342407].
- Klien BA, Olwin JH. A survey of the pathogenesis of retinal venous occlusion, emphasis upon choice of therapy and an analysis of the therapeutic results in fifty-three patients. AMA Arch Ophthalmol 1956; 56:207-47. [PMID: 13354061].
- Koyanagi Y. Die pathologische Anatomie und Pathogenese des Kreuzungsphänomens der NetzhautgefäÙe bei Hochdruck. Albrecht Von Graefes Arch Ophthalmol 1936; 135:526-36. .
- Sallmann L. Zur Anatomie der GefäÙkreuzungen am Augenhintergrund. Albrecht Von Graefes Arch Ophthalmol 1937; 137:619-35. .

9. Feltgen N, Hansen LL, Agostini H. Treatment of Retinal Vein Occlusion - Is There Still a Role for Vitreoretinal Surgery? *Klin Monatsbl Augenheilkd* 2017; 234:1103-8. [PMID: 28683483].
10. Khayat M, Lois N, Williams M, Stitt AW. Animal Models of Retinal Vein Occlusion. *Invest Ophthalmol Vis Sci* 2017; 58:6175-92. [PMID: 29222552].
11. Martin G, Conrad D, Cakir B, Schlunck G, Agostini HT. Gene expression profiling in a mouse model of retinal vein occlusion induced by laser treatment reveals a predominant inflammatory and tissue damage response. *PLoS One* 2018; 13:e0191338. [PMID: 29529099].
12. Cehofski LJ, Kruse A, Alsing AN, Nielsen JE, Pedersen S, Kirkeby S. u. aIntravitreal bevacizumab upregulates trans-thyretin in experimental branch retinal vein occlusion. *Mol Vis* 2018; 24:759-66. [PMID: 30581282].
13. McAllister IL, Vijayasekaran S, Yu D-Y. Intravitreal teneceplase (metalyse) for acute management of retinal vein occlusions. *Invest Ophthalmol Vis Sci* 2013; 54:4910-8. [PMID: 23766477].
14. Pournaras CJ, Petropoulos IK, Pournaras J-AC, Stangos AN, Gilodi N, Rungger-Brändle E. The rationale of retinal endovascular fibrinolysis in the treatment of retinal vein occlusion: from experimental data to clinical application. *Retina* 2012; 32:1566-73. [PMID: 22466460].
15. Bhutto IA, Amemiya T. Corrosion cast demonstration of retinal vasculature of normal Wistar-Kyoto rats. *Acta Anat (Basel)* 1995; 153:290-300. [PMID: 8659253].
16. Simoens P, De Schaepdrijver L, Lauwers H. Morphologic and clinical study of the retinal circulation in the miniature pig. A: Morphology of the retinal microvasculature. *Exp Eye Res* 1992; 54:965-73. [PMID: 1521587].
17. Rogers S, McIntosh RL, Cheung N, Lim L, Wang JJ, Mitchell P. u. aThe prevalence of retinal vein occlusion: pooled data from population studies from the United States, Europe, Asia, and Australia. *Ophthalmology* 2010; 117:313-319.e1. [PMID: 20022117].
18. Hamid S, Mirza SA, Shokh I. Anatomic pattern of arteriovenous crossings in branch retinal vein occlusion. *J Pak Med Assoc* 2008; 58:233-6. [PMID: 18655397].
19. Zhao J, Sastry SM, Sperduto RD, Chew EY, Remaley NA. Arteriovenous crossing patterns in branch retinal vein occlusion. The Eye Disease Case-Control Study Group. *Ophthalmology* 1993; 100:423-8. [PMID: 8460014].
20. Duker JS, Brown GC. Anterior location of the crossing artery in branch retinal vein obstruction. *Arch Ophthalmol* 1989; 107:998-1000. [PMID: 2751472].
21. Sekimoto M, Hayasaka S, Setogawa T. Type of arteriovenous crossing at site of branch retinal vein occlusion. *Jpn J Ophthalmol* 1992; 36:192-6. [PMID: 1513066].
22. Staurenghi G, Lonati C, Aschero M, Orzalesi N. Arteriovenous crossing as a risk factor in branch retinal vein occlusion. *Am J Ophthalmol* 1994; 117:211-3. [PMID: 8116749].
23. Feist RM, Ticho BH, Shapiro MJ, Farber M. Branch retinal vein occlusion and quadratic variation in arteriovenous crossings. *Am J Ophthalmol* 1992; 113:664-8. [PMID: 1598957].
24. Weinberg DV, Egan KM, Seddon JM. Asymmetric distribution of arteriovenous crossings in the normal retina. *Ophthalmology* 1993; 100:31-6. [PMID: 8433824].
25. Jefferies P, Clemett R, Day T. An anatomical study of retinal arteriovenous crossings and their role in the pathogenesis of retinal branch vein occlusions. *Aust N Z J Ophthalmol* 1993; 21:213-7. [PMID: 8148137].

Articles are provided courtesy of Emory University and the Zhongshan Ophthalmic Center, Sun Yat-sen University, P.R. China. The print version of this article was created on 15 October 2020. This reflects all typographical corrections and errata to the article through that date. Details of any changes may be found in the online version of the article.